

Shot-Noise-Driven Escape in Hysteretic Josephson Junctions

J. P. Pekola,¹ T. E. Nieminen,¹ M. Meschke,¹ J. M. Kivioja,¹ A. O. Niskanen,^{1,2} and J. J. Vartiainen¹

¹*Low Temperature Laboratory, Helsinki University of Technology, P.O. Box 3500, 02015 TKK, Finland*

²*VTT Information Technology, Microsensing, P.O. Box 1207, 02044 VTT, Finland*

(Received 18 February 2005; published 3 November 2005)

We have measured the influence of shot noise on hysteretic Josephson junctions initially in the macroscopic quantum tunneling regime. The escape threshold current into the resistive state decreases monotonically with increasing average current through the scattering conductor, which is another tunnel junction. Escape is predominantly determined by excitation due to the wideband shot noise. This process is equivalent to thermal activation (TA) over the barrier at effective temperatures up to about 4 times the critical temperature of the superconductor. The presented TA model is in excellent agreement with the experimental results.

DOI: 10.1103/PhysRevLett.95.197004

PACS numbers: 85.25.Cp, 05.40.-a, 72.70.+m

Shot noise and full counting statistics (FCS) in mesoscopic conductors are currently intensively studied because such measurements yield fingerprints of conduction mechanisms of these scatterers [1–4]. Yet direct measurements of the second and higher moments of current or voltage are typically much more difficult and prone to errors as compared to the measurement of dc transport properties. This is because, in order to extract information about fluctuations, one generally needs to perform high frequency measurements on remotely connected samples at cryogenic temperatures, which is, in practice, a non-trivial task. Therefore, detectors of noise and FCS that operate directly on-chip near the noise source are of great importance. A recently proposed readout device of these fluctuations is a Josephson junction (JJ) threshold detector [5,6]. A mesoscopic nonhysteretic Josephson junction in the Coulomb blockade regime is another choice [7–9].

The dynamics of the JJ can be described as that of a phase (φ) particle in a tilted cosine potential; see Fig. 1. Under the influence of equilibrium environment fluctuations at low temperatures, the particle resides in the quantum mechanical ground state, from where the escape mechanism is tunneling [macroscopic quantum tunneling (MQT)] through the barrier. At higher temperatures, it assumes a nearly thermal population of the states, and the escape mechanism is predominantly thermal activation (TA) over the barrier top. Below we discuss the regime where excited states are not accessed by the influence of the thermal noise of the dissipative environment, which is an appropriate assumption based on our present measurements in the absence of shot noise and those of Ref. [10] in the same setup at low temperatures.

The influence of noisy current on escape characteristics is typically considered in two limits: (i) adiabatic (quasi-stationary) regime, where fluctuations of bias current that change the tilt of the cosine potential are so slow and weak that the phase particle remains in the ground state of the metastable well, and the escape rate is dictated by MQT from this varying ground state [6,11], or (ii) (nearly) reso-

nance excitation limit, where most of the escape events are consequences of shot-noise-driven excitations of the phase particle into higher levels in the well. Because of the high frequency resonance character of our on-chip circuit, it turns out that the latter approach is more appropriate in describing the dynamics of the detector in this case.

In this Letter, we show that a hysteretic Josephson junction in the MQT regime can measure high frequency current fluctuations generated by a mesoscopic scatterer in nonequilibrium. We present a model in which the noisy current excites the phase particle in a metastable, nearly parabolic well out from the ground state, and, subsequently, the particle escapes from the well. This occurs via thermal activation at an equivalent temperature of the phase particle, which is determined by the competition between shot-noise excitation and relaxation due to the

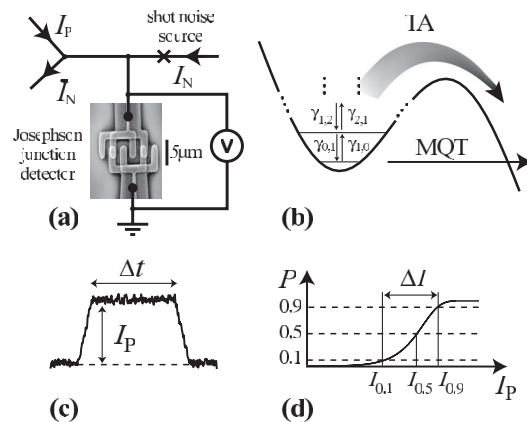


FIG. 1. (a) Measurement configuration. A split JJ in MQT regime measures the current fluctuations due to the shot noise of the scattering junction in the right arm. (b) Processes leading to escape from the zero-voltage (supercurrent) state into the resistive state. (c) Sketch of current pulses I_P , with superimposed noise of I_N , and (d) the associated escape characteristics. The central quantities relating to the pulses and escape histograms have been indicated in the figure.

dissipative environment. This model is in excellent agreement with our experimental results, and we are able to investigate Josephson phase dynamics up to effective temperatures which are about 4 times higher than the critical temperature of the superconductor. This is the effective temperature responsible for phase dynamics: The electrons and lattice of the superconductor remain, however, essentially at their base temperature.

Our measurement configuration with an electron micrograph of a split JJ detector is shown in Fig. 1. In a typical experiment, two currents I_N and I_P are injected into the circuit through large resistances ($> 1 \text{ M}\Omega$) at room temperature. Current I_N is applied constantly, and it runs through another tunnel junction at a distance of $120 \mu\text{m}$ from the detector. This junction plays the role of the shot-noise source in the circuit. The dc component of this current, \bar{I}_N , returns through a long (3 mm) and narrow (width $2 \mu\text{m}$) superconducting line such that no dc current due to I_N passes through the detector. We verify this balance frequently during the measurements. Thus, only the fluctuations of I_N are admitted through the detector. We probe these fluctuations by applying repeatedly trapezoidal current pulses of height I_P through the detector as shown in Fig. 1(c). These pulses are slow, typically $10 \mu\text{s}$ – 10 ms long and with long transient times at the beginning and at the end of the pulse to secure adiabatic response to them. Typically, 1000 pulses at each value of I_P are repeated, and the escape probability $P(I_P)$ is obtained as the fraction of those pulses that lead to escape from the supercurrent state.

In the common resistively and capacitively shunted junction model of a JJ, the phase particle in the tilted cosine potential is either trapped and oscillating in one of the wells or, alternatively, it runs down the potential [12]. The latter regime is called the resistive state. The measurable quantities, i.e., current I and voltage V , are related to φ via the Josephson equations: $I = I_C \sin\varphi$ and $2eV = \hbar \frac{d\varphi}{dt}$, where $I_C = \frac{2e}{\hbar} E_J$ is the critical current of the junction and E_J is its Josephson coupling energy. The quality factor $Q \equiv \omega_p RC$ is assumed to be $Q \gg 1$ to assure hysteretic dynamics. This means that, once the particle leaves the well, it runs freely such that the voltage across the junction is close to twice the energy gap of the superconductor, and it can be retrapped to the zero-voltage supercurrent state only when current is lowered virtually to zero. Here R is the resistive shunt of the junction, C is the parallel capacitance, and $\omega_p \equiv \sqrt{8E_J E_C q_0} / \hbar$ is the plasma frequency, where $E_C = e^2/2C$ and $q_0 = \sqrt{2(1 - I/I_C)}$. Quantum mechanically, the phase particle has energy states in the nearly parabolic wells, with energies close to those of a harmonic oscillator: $E_n \approx (n + 1/2)\hbar\omega_p$.

Because of the nearly harmonic potential, transitions between the neighboring levels are dominating. The rates of these transitions [see Fig. 1(b)] are determined by the spectral density $S_I(\omega) = \int_{-\infty}^{\infty} \langle \delta I(t) \delta I(0) \rangle \exp(i\omega t) dt$ of the current noise $\delta I(t)$ at the corresponding level separation

$\omega = \omega_{j,j-1}$ as $\gamma_{j,j-1} \approx (j/2\hbar\omega_{j,j-1}C)S_I(-\omega_{j,j-1})$ and $\gamma_{j-1,j} \approx (j/2\hbar\omega_{j,j-1}C)S_I(+\omega_{j,j-1})$ for excitation and relaxation, respectively [7,13]. The noise spectrum has two contributions: one due to the equilibrium environment S_I^{env} and the other due to shot noise S_I^{shot} , which add incoherently: $S_I = S_I^{\text{env}} + S_I^{\text{shot}}$. At low temperature $k_B T \ll \hbar\omega_p$, the thermal excitation is strongly suppressed, $S_I^{\text{env}}(-\omega_{j,j-1}) \rightarrow 0$, and the relaxation is due to zero point fluctuations, $S_I^{\text{env}}(+\omega_{j,j-1}) \rightarrow 2\hbar\omega_{j,j-1} \text{Re}Y(\omega_{j,j-1})$, where $Y(\omega)$ is the admittance of the circuit surrounding the Josephson junction. The shot noise responsible for transitions in the Josephson junction can be described as $S_I^{\text{shot}}(\pm\omega_{j,j-1}) = Fe\bar{I}_N$. Here \bar{I}_N is the average current through the scatterer, and F is the ‘‘Fano factor’’ of the noise source and the circuit surrounding the JJ, at the frequency corresponding to level separation. Factor F can be calculated for a known experimental circuit. Here we determine it experimentally as a fit parameter. It would be unity in the case of Poissonian tunnel junction source [1] and if all the noise current would run through the detector junction. Combining the results above, we have

$$\gamma_{j,j-1} \approx \frac{jFe\bar{I}_N}{2\hbar\omega_{j,j-1}C} \quad (1)$$

and

$$\gamma_{j-1,j} \approx \frac{jFe\bar{I}_N}{2\hbar\omega_{j,j-1}C} + \frac{j\omega_{j,j-1}}{Q}. \quad (2)$$

The level dynamics described by Eqs. (1) and (2) can be described by the equivalent temperature T^* and effective quality factor Q^* by requesting $\gamma_{j,j-1} \equiv j(\omega_{j,j-1}/2Q^*) \times [\coth(\hbar\omega_{j,j-1}/2k_B T^*) - 1]$ and $\gamma_{j-1,j} \equiv j(\omega_{j,j-1}/2Q^*) \times [\coth(\hbar\omega_{j,j-1}/2k_B T^*) + 1]$. This yields $Q^* = Q$ and, with $\omega_{j,j-1} \approx \omega_p$,

$$k_B T^* \approx \frac{\hbar\omega_p}{2 \text{arcoth}(1 + QFe\bar{I}_N/\hbar\omega_p^2 C)}. \quad (3)$$

In the following, we make use of standard results of the influence of temperature on the decay from a cubic metastable well (see, e.g., Ref. [14]) and note that, formally, we do not need to make a distinction of whether the temperature is determined by the equilibrium environment (T) or by the combination of this environment and shot noise (T^*). We can infer that (classical) thermal activation is the dominant escape mechanism, provided $T^* > T_0 \equiv \hbar\omega_p/2\pi k_B$. This yields a condition for the validity of the TA model: $\text{arcoth}(1 + QFe\bar{I}_N/\hbar\omega_p^2 C)/\pi < 1$. This is fulfilled at all currents \bar{I}_N that were employed in the experiments, as we will show below. With this procedure, it is then straightforward to obtain the switching probability of the threshold detector, in the limit of many levels in the well, as $P(\bar{I}_P) = 1 - \exp(-\Gamma\Delta t)$. Here $\Gamma = (\omega_p/2\pi) \times \exp(-\Delta U/k_B T^*)$ is the standard TA escape rate, Δt is

the length of the current pulse, and $\Delta U = 4\sqrt{2}E_J(1 - I_p/I_C)^{3/2}/3$ is the height of the potential barrier at the particular bias point I_p . The expressions above allow us to evaluate the position $I_{0.5}$ and the width $\Delta I = I_{0.9} - I_{0.1}$ of the escape threshold, where I_x is defined by $P(I_x) \equiv x$; see Fig. 1(d). These approximate results were compared to those obtained by full level dynamics calculation (LDC) [15] numerically. The overall agreement between the two results is good, although $I_{0.5}$ from the two methods can deviate by a few percent depending on how one obtains the level positions and widths near the top of the barrier in LDC.

In the limit of large noise currents, $\bar{I}_N \gg \hbar\omega_p^2 C/(QFe)$, we obtain $T^* \approx QFe\bar{I}_N/(2k_B\omega_p C)$, which can be written in a more familiar looking form $T^* \approx Fe\bar{I}_N/(2k_B/R)$. This is a valid approximation in a wide range of experimental parameters. The expressions of TA escape and the current dependence of the barrier height combined with this approximate expression of T^* finally allow us to approximate $I_{0.5}$ as

$$I_{0.5}/I_C \approx 1 - \left(\frac{3}{4\sqrt{2}}\right)^{2/3} \left[\ln\left(\frac{\omega_p \Delta t}{2\pi\kappa_{0.5}}\right) \right]^{2/3} \left(QF \frac{E_C}{E_J} \frac{\bar{I}_N}{e\omega_p} \right)^{2/3} \quad (4)$$

and ΔI , assuming $\omega_p \Delta t \gg 1$, as

$$\Delta I/I_C \approx \frac{\ln(\kappa_{0.9}) - \ln(\kappa_{0.1})}{[12 \ln(\frac{\omega_p \Delta t}{2\pi})]^{1/3}} \left(QF \frac{E_C}{E_J} \frac{\bar{I}_N}{e\omega_p} \right)^{2/3}. \quad (5)$$

Here $\kappa_x \equiv -\ln(1-x)$.

We report on data of two samples, A and B, which were fabricated by standard electron beam lithography and shadow evaporation with aluminum as the superconductor. The samples were measured via adequately filtered signal lines in dilution refrigerators at bath temperatures of 30 mK—1 K. Sample A had a split JJ detector and one scattering junction as in the scheme of Fig. 1. Sample B had a single JJ as a detector, and it had two scattering junctions located symmetrically with respect to the detector (at a distance of 120 μm) and with respect to *two* long injection lines. In this sample, the two scattering junctions were made intentionally very different to check the invariance of the results with respect to junction properties. The parameters of the two samples are listed in Table I.

Data in Fig. 2(a) show results of a control experiment on sample B at the base temperature $T \approx 30$ mK, where the trapezoidal pulse current I was injected through (i) one of

the long injection lines, (ii) through scatterer 1, and (iii) through scatterer 2. The histogram of case (i) lies at higher currents than those of (ii) and (iii), which in turn practically overlap with each other. This demonstrates that shot noise tends to push the threshold towards lower values of current, as predicted, e.g., by Eq. (4). Furthermore, these data demonstrate that the noise is predominantly, and equally in (ii) and (iii), generated by the scattering tunnel junctions. The calculated lines run through the corresponding experimental histograms assuming MQT without any noise in (i) and TA with T^* evaluated from Eq. (3) with $QF = 5$ in (ii) and (iii). The latter value is realistic in terms of the expected $Q \approx 10$ [10] and $F \leq 1$.

Figure 2(b) shows data on sample B at $T = 40$ mK. The threshold current $I_{0.5}$, i.e., the pulse current at which the switching probability is 50%, has been plotted as a function of \bar{I}_N through scatterer 2. The data, shown by solid symbols, follow the prediction of the model presented above, again with $QF = 5$. The initial plateau in the experimental data below $I_N \approx 100$ nA arises because the scattering junction is not in the linear quasiparticle tunneling regime here. The inset in Fig. 2(b) shows the IV curve of this junction. In Fig. 2(c) we plot, in addition to similar data as in Fig. 2(b), the equivalent temperature T^* in the measurement of sample A when current \bar{I}_N is varied between 2 and 8 μA . There are two interesting points to note: (i) We are able to study Josephson dynamics of the JJ up to $T^* \approx 5$ K, about 4 times above the critical temperature T_C

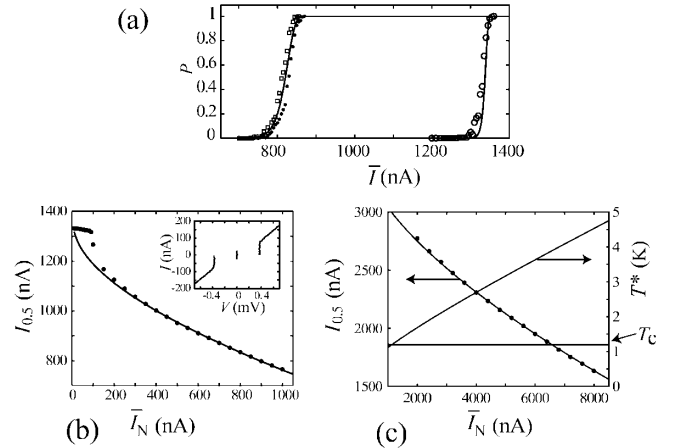


FIG. 2. Histogram positions under shot-noise injection. (a) Escape histograms of sample B when current pulses have been injected through the long injection line (open circles) and through the two noise sources (source 1, squares; source 2, solid circles), respectively. The lines are the corresponding theoretical results. (b) Experimental results (circles) on the switching threshold current $I_{0.5}$ against the average current \bar{I}_N through scatterer 2 in sample B. The solid line is again the result of the used theoretical model. The inset shows the IV curve of the noise source. (c) Similar data as in (b) but for sample A. The rising curve shows the equivalent temperature T^* , which ranges from 2 to 5 K. Pulse length was $\Delta t = 800$ μs .

TABLE I. Parameters of the two samples.

| Sample | I_C detector | C detector | I_C scatterer | C scatterer |
|--------|-------------------|--------------|------------------------|------------------------|
| A | 3.9 μA | 230 fF | 600 nA | 40 fF |
| B | 1.5 μA | 230 fF | 15 nA (1) 90 nA (2) | 10 fF (1) 40 fF (2) |

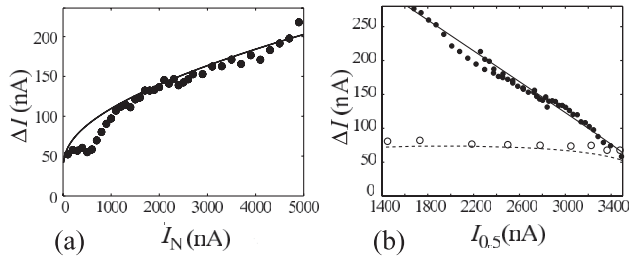


FIG. 3. The width of the histograms, ΔI , when shot noise and thermal noise are applied. (a) The width against the average current \bar{I}_N through the scatterer. The dots are the experimental results and the solid line is the result of the theoretical model. (b) ΔI vs $I_{0.5}$ under two different experimental conditions. The solid circles are data with elevated shot-noise temperature T^* , whereas the open circles are with variable bath temperature T . The solid line is the result of the thermal activation model with a constant energy gap, and the dashed line takes into account the suppression of the BCS gap [16] in the measurement with increased T .

of aluminum. (ii) At all currents employed, we are well above the threshold $T_0 \approx 0.3$ K of thermal activation.

Figure 3(a) shows the width of the switching threshold, ΔI , of sample A. Again, the experimental (circles) and theoretical (line) results are in good agreement between each other using the same fit parameters as in Fig. 2. In Fig. 3(b), data on switching of sample A has been plotted in two different experimental conditions, in each case as ΔI vs $I_{0.5}$. The open circles are data where the bath (lattice) temperature has been varied by heating the sample stage to several temperatures T in the range 0.03—1 K. The solid circles are data taken at the base temperature $T \approx 30$ mK but varying the equivalent temperature T^* , injecting different levels of \bar{I}_N . The line closely following the latter data is from the thermal activation model. At first sight, it is surprising that the truly thermal data (open circles) fall far below this line and the other set of data. This is, however, accounted for by the fact that, when increasing the bath temperature close to T_C of aluminum (~ 1.2 K), the BCS energy gap is progressively diminishing, thus leading to decrease of the critical current. The line following closely this data set is obtained by using the very same thermal activation model but by taking into account suppression of the BCS gap due to temperature T [16]. This figure thus demonstrates that our thermal activation model is in good agreement with the shot-noise data and that it is indeed possible, by promoting shot noise, to study Josephson dynamics at effective noise temperatures higher than T_C without suppressing superconductivity.

Finally, there are a few more topics to address. We found out that the adiabatic models of rocking slowly the current bias of the JJ do not account for our observations on shot noise: The adiabatic models, involving no excitations,

predict exponential dependence in variance of the current of the tunneling rate from the ground state [6,11]. Our experimental results demonstrate, however, much weaker dependence, which we derived in this Letter. The (nearly) resonant model works in this case because the high frequency shot noise can pass the detector junction. Furthermore, we expect that the low frequency noise ($\ll 1$ GHz) does not run through the detector junction because of the high-pass character of the setup. Note that at dc we suppress the detector current due to I_N totally. The second issue is the assessment of a MQT detector as an absolute noise detector. Based on the invariance of the obtained results, especially in terms of results on different scatterers on the same sample [see Fig. 2(a)], we suggest that this kind of a detector could be made into an absolute on-chip detector of Fano factors [1], and noise in general, by careful tailoring of the circuit surrounding the JJ and by measuring Q independently.

We thank T. Heikkilä, T. Ojanen, E. Sonin, and A. Savin for useful discussions and H. Grabert and D. Esteve for their insightful comments at an early stage of this work. We acknowledge Academy of Finland for financial support.

-
- [1] Y.M. Blanter and M. Büttiker, Phys. Rep. **336**, 1 (2000).
 - [2] *Quantum Noise in Mesoscopic Physics*, edited by Yu. V. Nazarov (Kluwer, Dordrecht, 2003).
 - [3] L. S. Levitov, H. W. Lee, and G. B. Lesovik, J. Math. Phys. (N.Y.) **37**, 4845 (1996).
 - [4] B. Reulet, J. Senzier, and D.E. Prober, Phys. Rev. Lett. **91**, 196601 (2003); B. Reulet, L. Spietz, C.M. Wilson, J. Senzier, and D.E. Prober, cond-mat/0403437.
 - [5] J. Tobiska and Yu. V. Nazarov, Phys. Rev. Lett. **93**, 106801 (2004).
 - [6] J.P. Pekola, Phys. Rev. Lett. **93**, 206601 (2004).
 - [7] R.J. Schoelkopf, A. A. Clerk, S.M. Girvin, K. W. Lehnert, and M.H. Devoret, in Ref. [2].
 - [8] R.K. Lindell *et al.*, Phys. Rev. Lett. **93**, 197002 (2004).
 - [9] T.T. Heikkilä, P. Virtanen, G. Johansson, and F.K. Wilhelm, Phys. Rev. Lett. **93**, 247005 (2004).
 - [10] J.M. Kivioja *et al.*, Phys. Rev. Lett. **94**, 247002 (2005).
 - [11] J.M. Martinis and H. Grabert, Phys. Rev. B **38**, 2371 (1988).
 - [12] Our junctions are biased at high enough I/I_C and their I_C is sufficiently large such that we can discuss the escape dynamics as if only one well exists [10].
 - [13] J.M. Martinis, S. Nam, J. Aumentado, K.M. Lang, and C. Urbina, Phys. Rev. B **67**, 094510 (2003).
 - [14] U. Weiss, *Quantum Dissipative Systems* (World Scientific, Singapore, 1999), 2nd ed.
 - [15] A.I. Larkin and Yu.N. Ovchinnikov, Zh. Eksp. Teor. Fiz. **91**, 318 (1986) [Sov. Phys. JETP **64**, 185 (1987)].
 - [16] M. Tinkham, *Introduction to Superconductivity* (McGraw-Hill, New York, 1996), 2nd ed.